TOR VERGATA
UNIVERSITÀ DEGLI STUDI DI ROMA

DMZ ENGINEERING

Finite Element-Based Thermo-Structural Optimization of an Internal Combustion Engine Intake Manifold

Candidate:
Gabriele Bortolotto

Supervisor:
Prof. Marco Evangelos Biancolini

Co-supervisors:
Ing. Riccardo Serenella
Prof. Lorenzo Bartolucci

Introduction

Thesis objective: thermo-structural optimization of a high-performance intake manifold.

- Development of a high-performance intake manifold
- Improved engine performance
- Design optimization through numerical simulations

Toyota **G16E-GTS** engine installed on a Yaris GR

- 3 in line cylinders
- Displacement: 1618 cc
- Power: 206 kW
- Torque: 345 Nm
- Material: aluminum alloy

Project objectives

- Geometric constraints: packaging requirements and ease of assembly
- Safety Factor = 1 under hydraulic proof testing conditions
- Safety Factor = 2 under nominal operating conditions.
- Safety Factor = 3 against buckling failure.
- 20% reduction in total manifold mass (from 1.6 Kg to 1.3 Kg).

Workflow


Reverse Engineering
3D CAD Modeling
Finite Element Analysis (FEA)
Parametric Optimization

Reverse Engineering

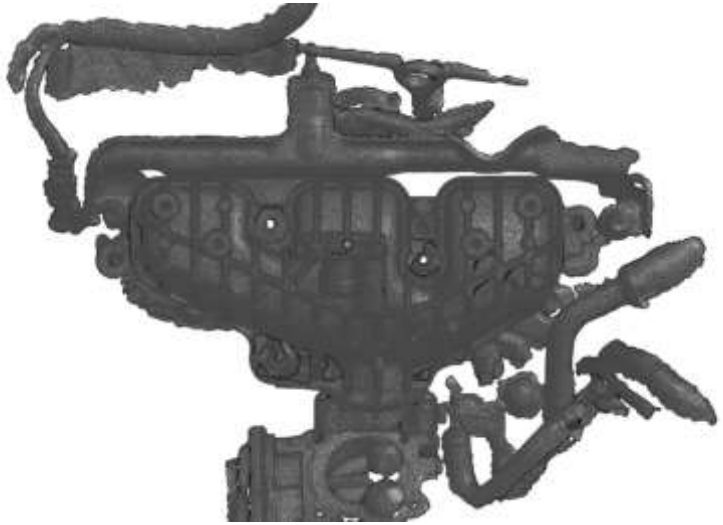

Process used to obtain a one-to-one digital model for design reference.

Scanned components:

- Intake manifold
- Cylinder head intake ports
- Engine bay without manifold

Marker application → 3D Scan → File STL

CAD 3D Modeling

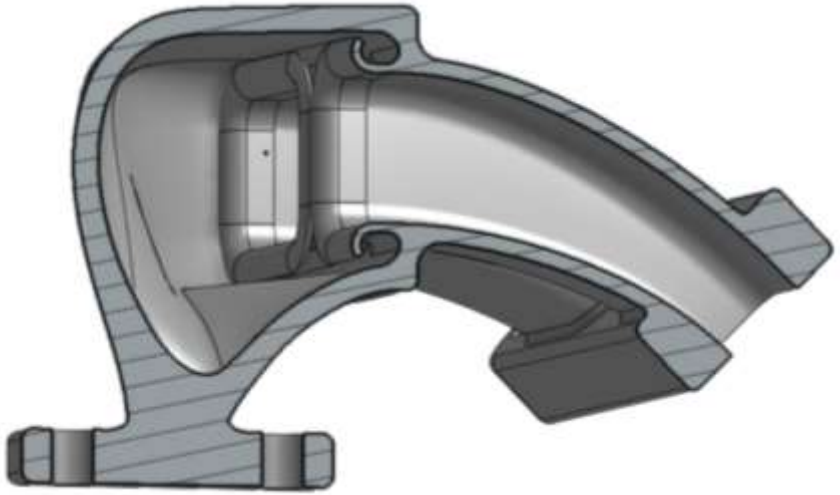

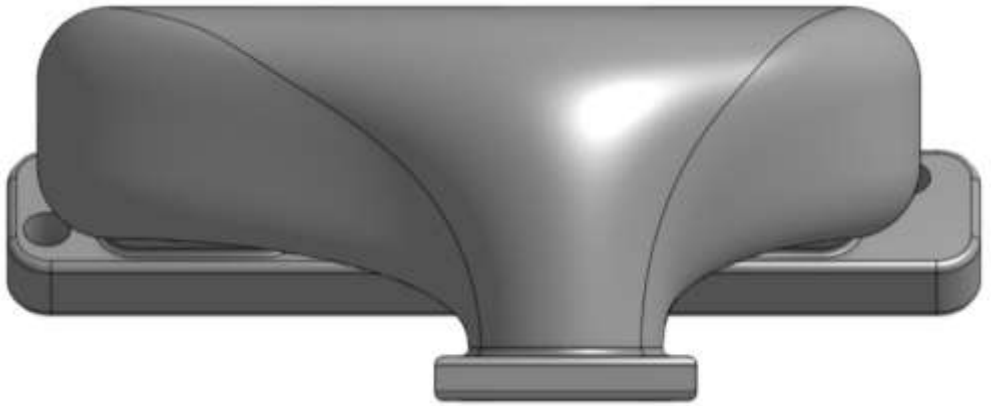

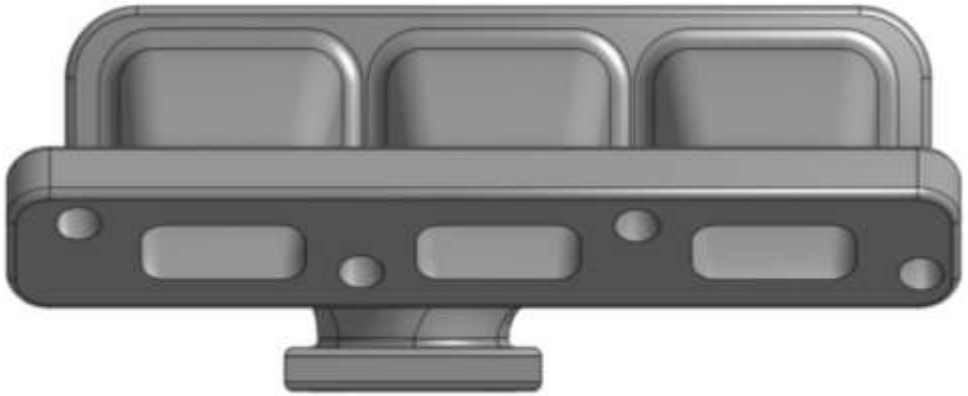

- Software: **Onshape**
- Parametric CAD modeling
- Extrude, loft and sweep features
- Runner thickness: 4.5 mm; plenum wall thickness: 7mm.
- Final design **validated through CFD** analysis

Structural loads evaluation

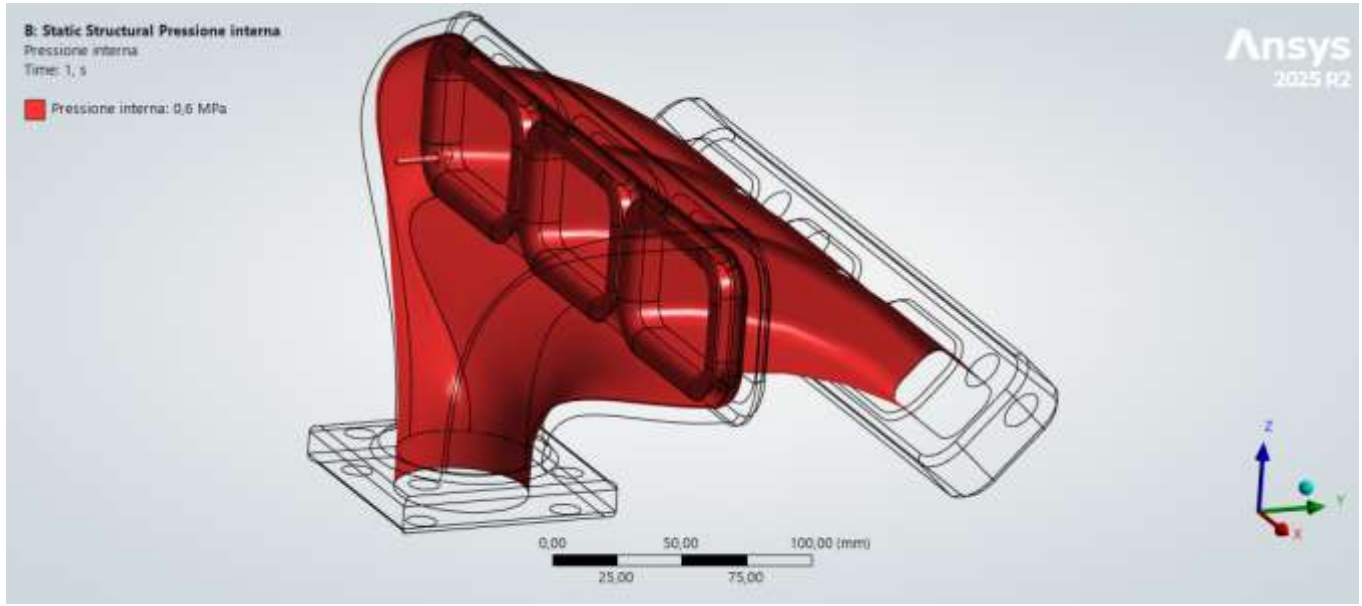

- Nominal load 2.8 Bar
- Maximum pressure 6 Bar
- Atmospheric pressure

A uniform internal pressure load was applied to all internal manifold surfaces.

A conservative pressure of 6 bar was considered to evaluate structural integrity.

Thermal loads evaluation

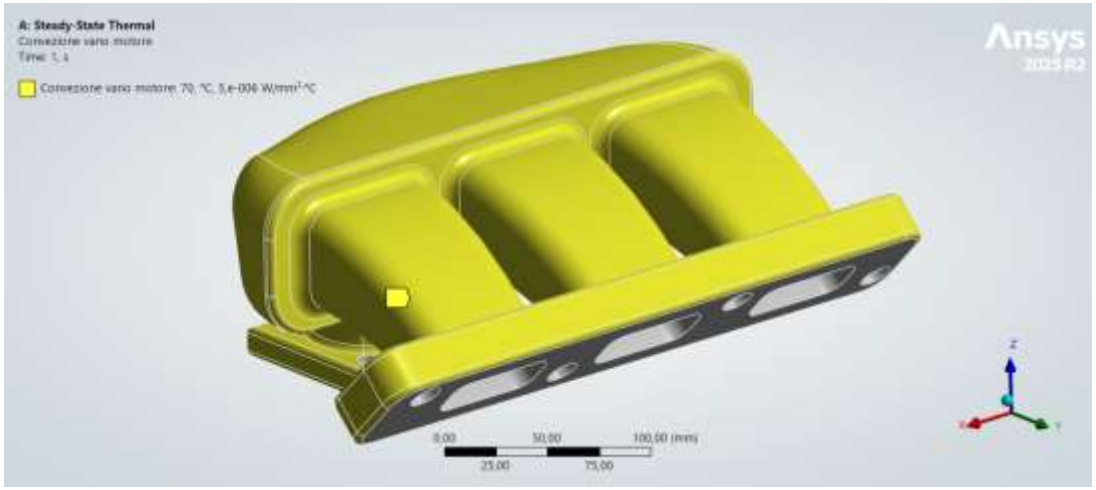

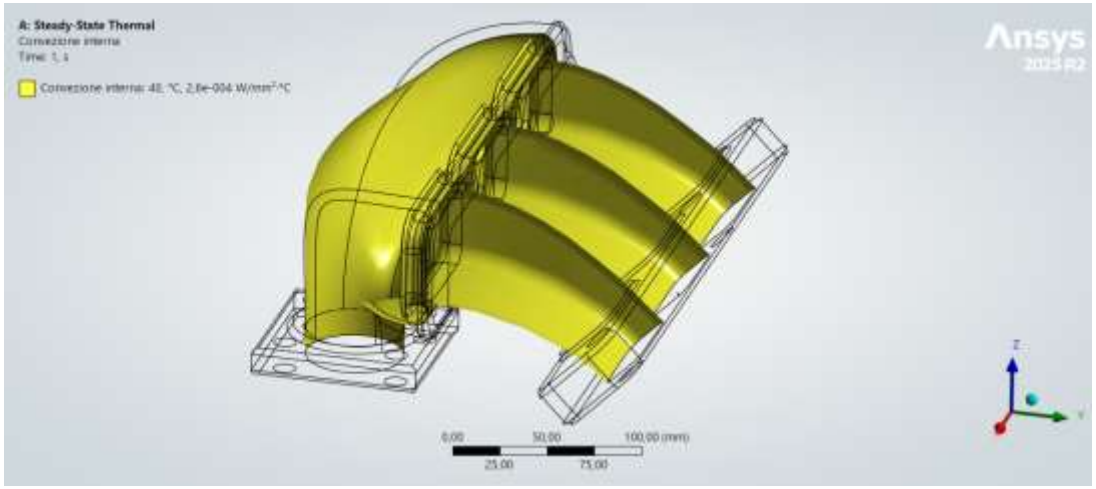

External convection	Internal convection
70°C	40°C
$5 \frac{W}{m^2 \, °C}$	$260 \frac{W}{m^2 \, °C}$

Internal convective heat transfer coefficient obtained from CFD simulations.

Boundary conditions

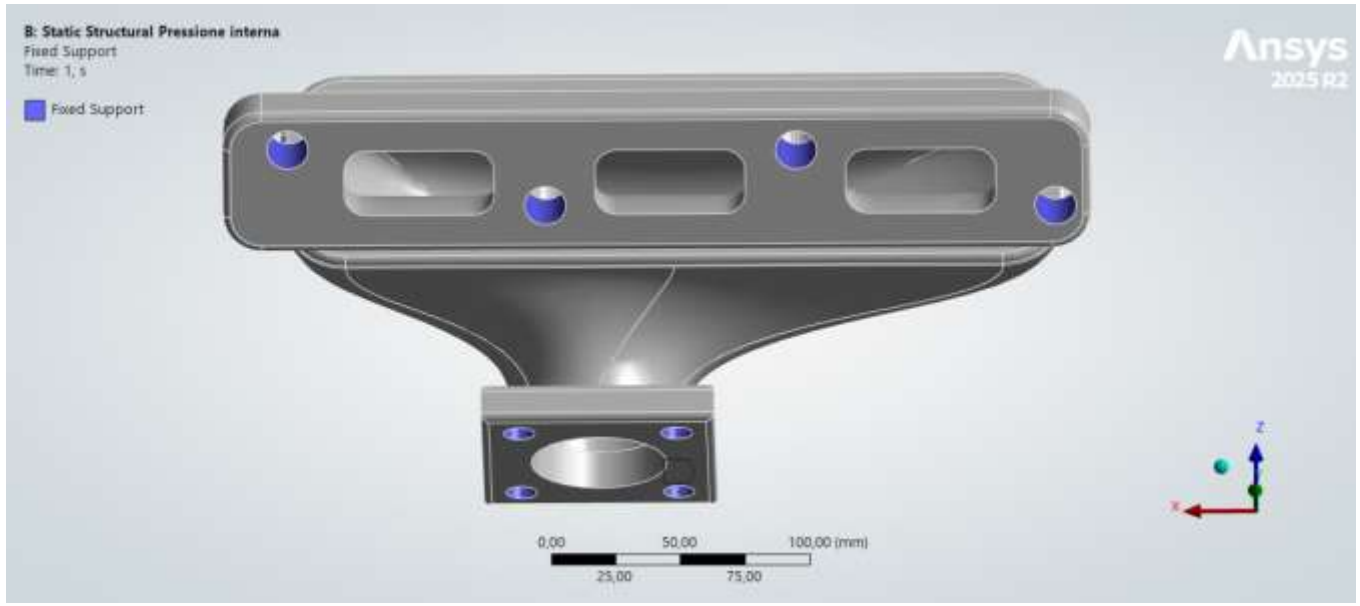

All nodes belonging to the mounting-hole geometry were constrained in all translational directions.

The six rigid-body modes were removed, ensuring that all displacements resulted exclusively from material deformation.

$$U_x = 0, \qquad U_y = 0, \qquad U_z = 0$$

Material properties

	PA12 MJF literature	Datasheet ANSYS
Density	1.01 x 10^{-6} kg/mm^3	1.01 x 10^{-6} kg/mm^3
Tensile strength	45÷50 MPa	49.7 MPa
Elastic modulus	1500÷1800 MPa	1207 MPa
Yield strength	40÷48 MPa	38.860 MPa
Ultimate tensile stress	45÷50 MPa	49.750 MPa
Poisson's ratio	0.40	0.41
Thermal conductivity	2.3 x 10^{-4} W/(mm °C)	2.5 x 10^{-4} W/(mm °C)
Melting temperature	182÷185°C	/
Crystallization temperature	147÷148°C	/

Thermal insulator

Excellent corrosion resistance

Isotropic under tensile loading

Anisotropic in bending

Thermoplastic material used in MJF 3D printing, elasto-plastic behavior with strain hardening.

Material properties

Due to the thermoplastic behavior of the material, it was necessary to import the variations of the mechanical properties as a function of temperature into the ANSYS environment.

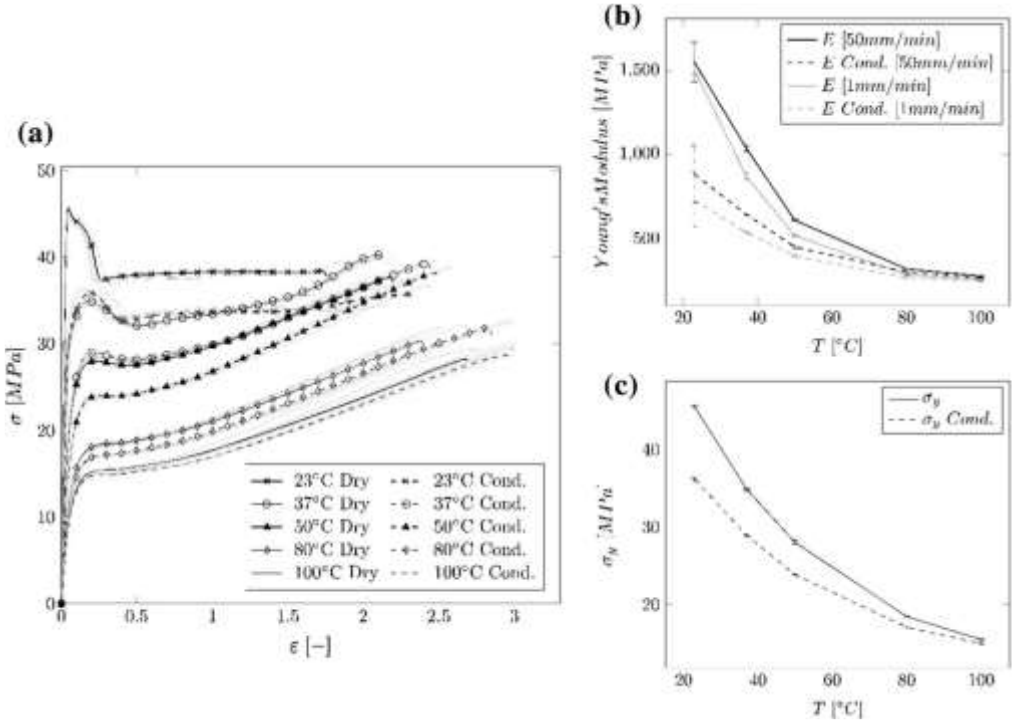

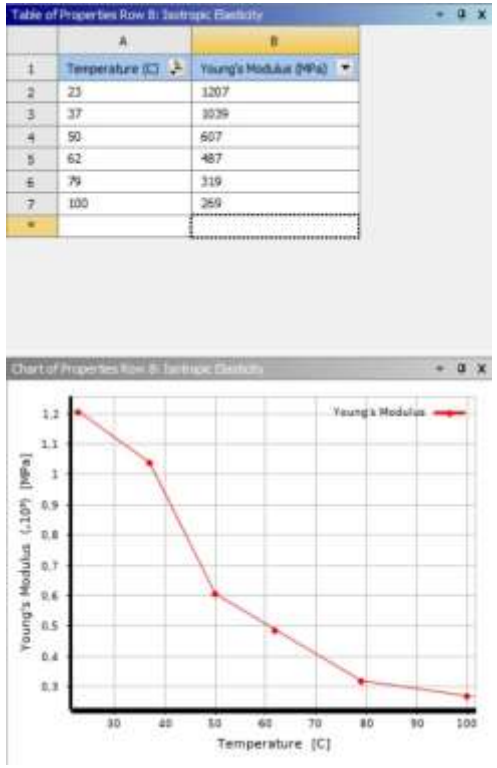

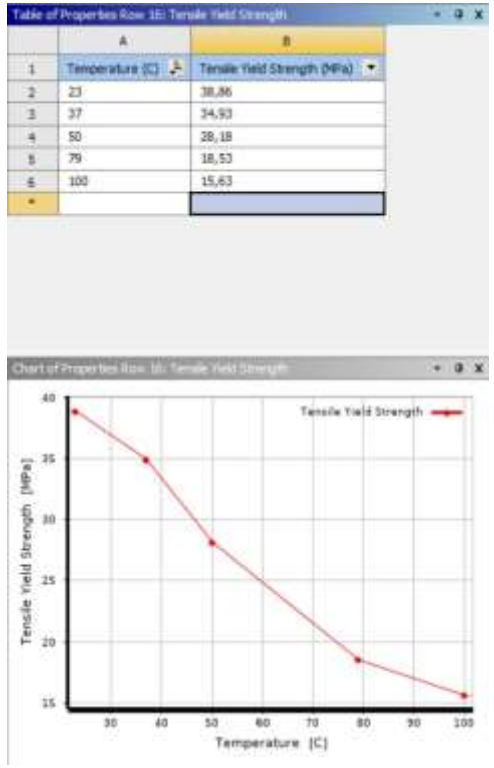

FEA Analysis

ANSYS Simulation Workflow

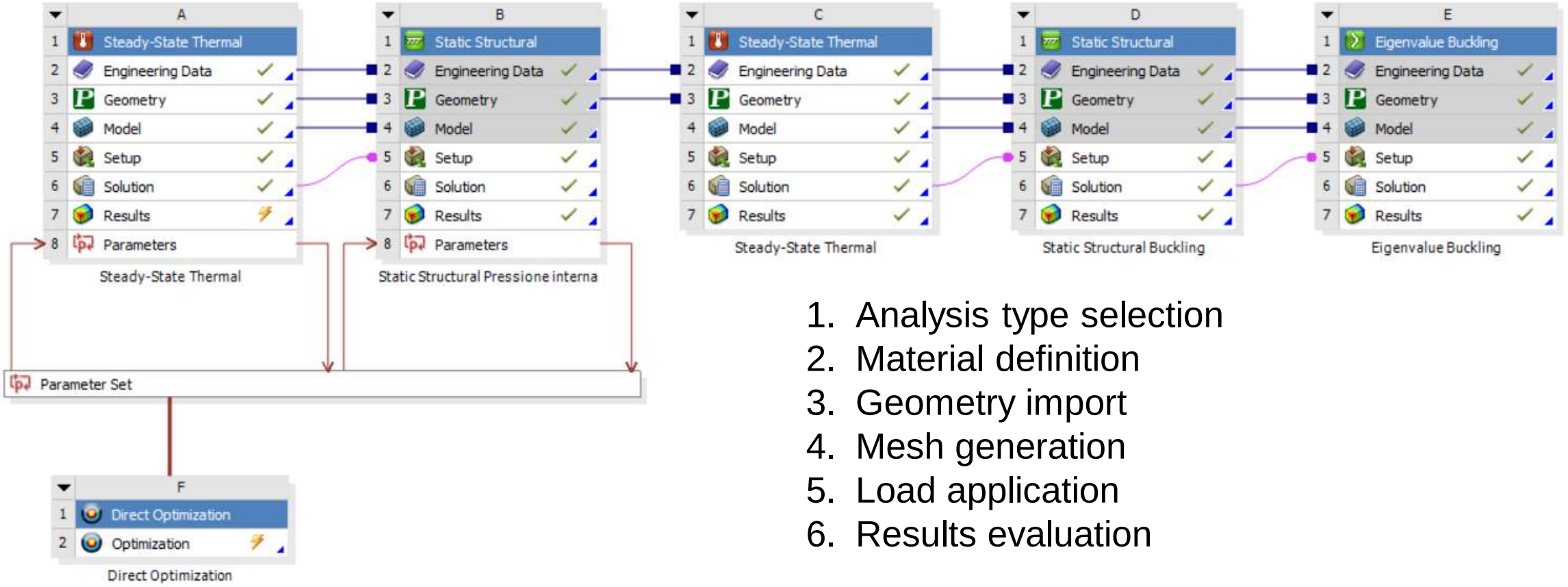

1. Analysis type selection
2. Material definition
3. Geometry import
4. Mesh generation
5. Load application
6. Results evaluation

Mesh generation and refinement

Test	Sizing fillets	Sizing plenum	Sizing runner	Nodes	Elements	Equivalent maximum stress	Variation
1	4 mm	9 mm	6.5 mm	$1.15\ 10^5$	67297	26.5 MPa	-14.79%
2	2 mm	7 mm	4.5 mm	$4.39\ 10^5$	$2.81\ 10^5$	27.5 MPa	-11.58%
3	1 mm	3.5 mm	2.25 mm	$1.77\ 10^6$	$1.19\ 10^6$	31.2 MPa	0.32%
4	0.8 mm	3.5 mm	2.25 mm	$2.52\ 10^6$	$1.71\ 10^6$	31.1 MPa	0.00%

The mesh was refined in regions characterized by high stress gradients and geometric details.

The third mesh configuration provided the best compromise between accuracy and computational cost.

Quadratic tetrahedral elements.

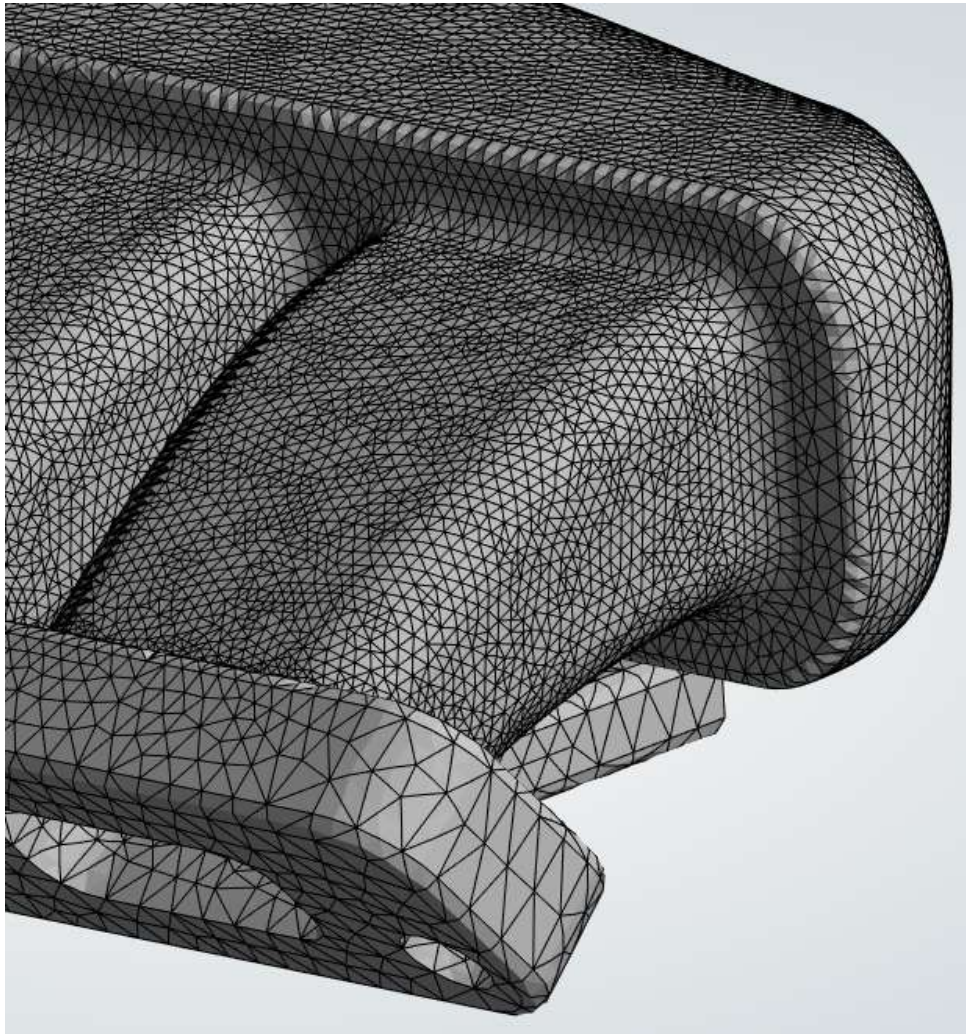

Baseline FEA Results

Temperature Distribution Analysis

- Maximum Temperature: 65.29 °C
- Minimum Temperature: 39.99 °C
- Average Temperature: 46.69 °C
- Average Runner Temperature: 43°C

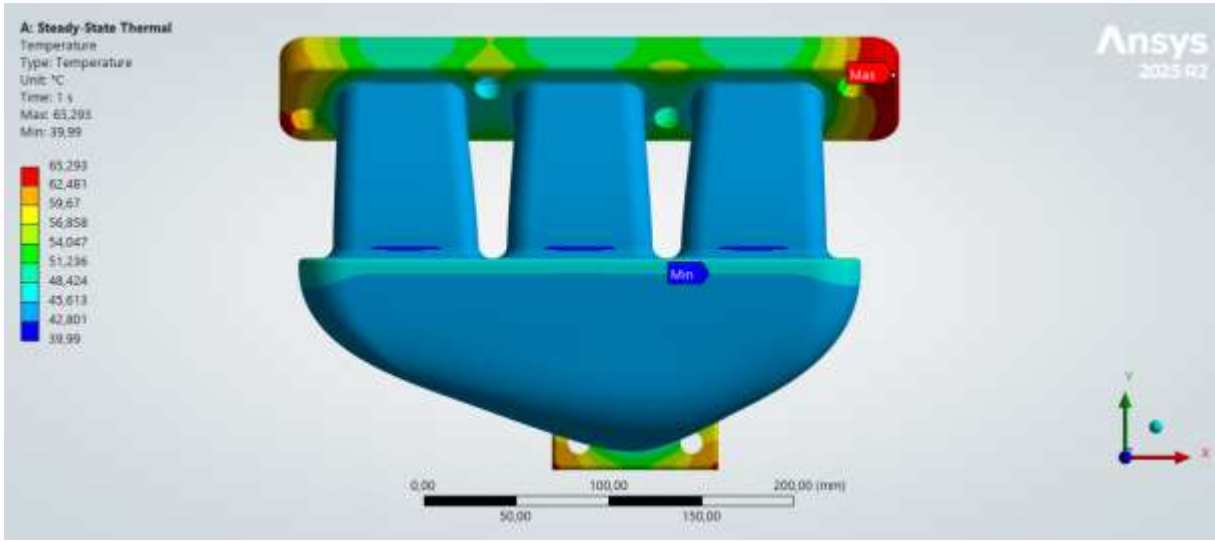

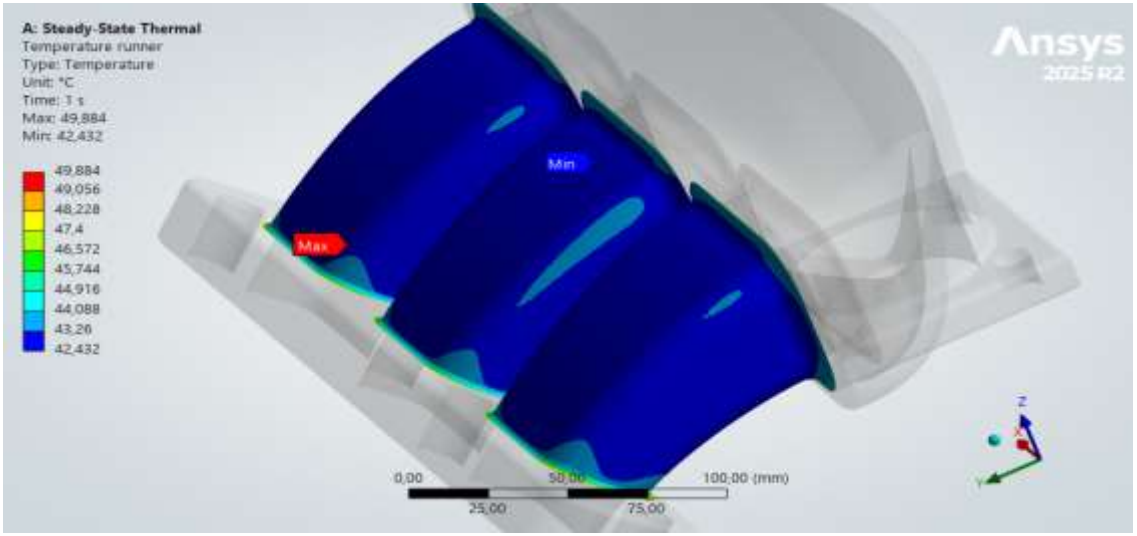

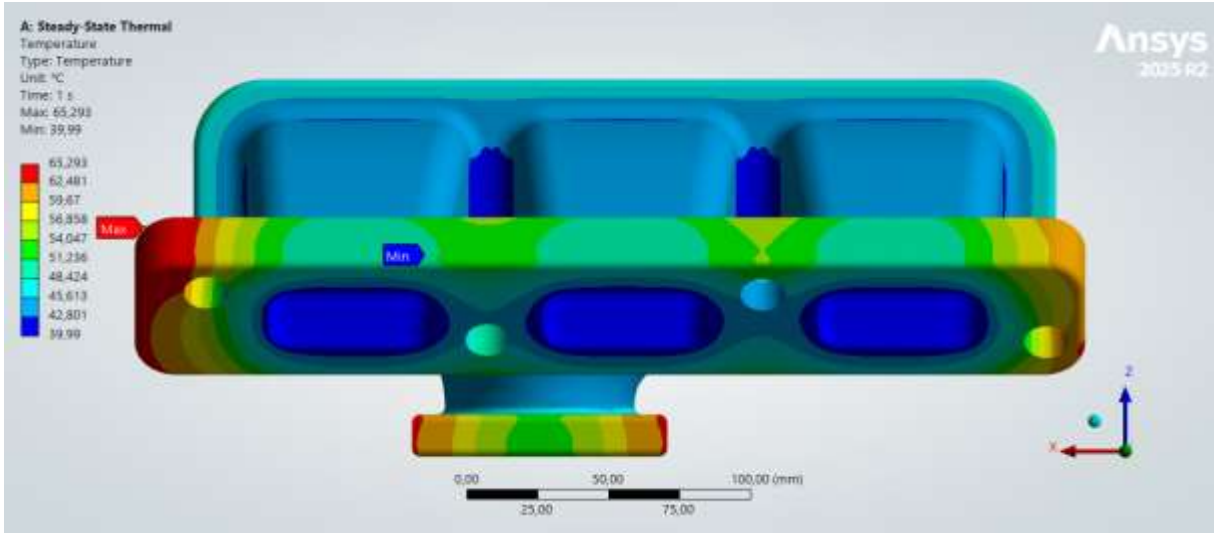

Baseline FEA Results

Stress Analysis: Internal Pressure of 6 bar

The flange-to-runner transition region experienced the highest stress concentration of 28.55 MPa.

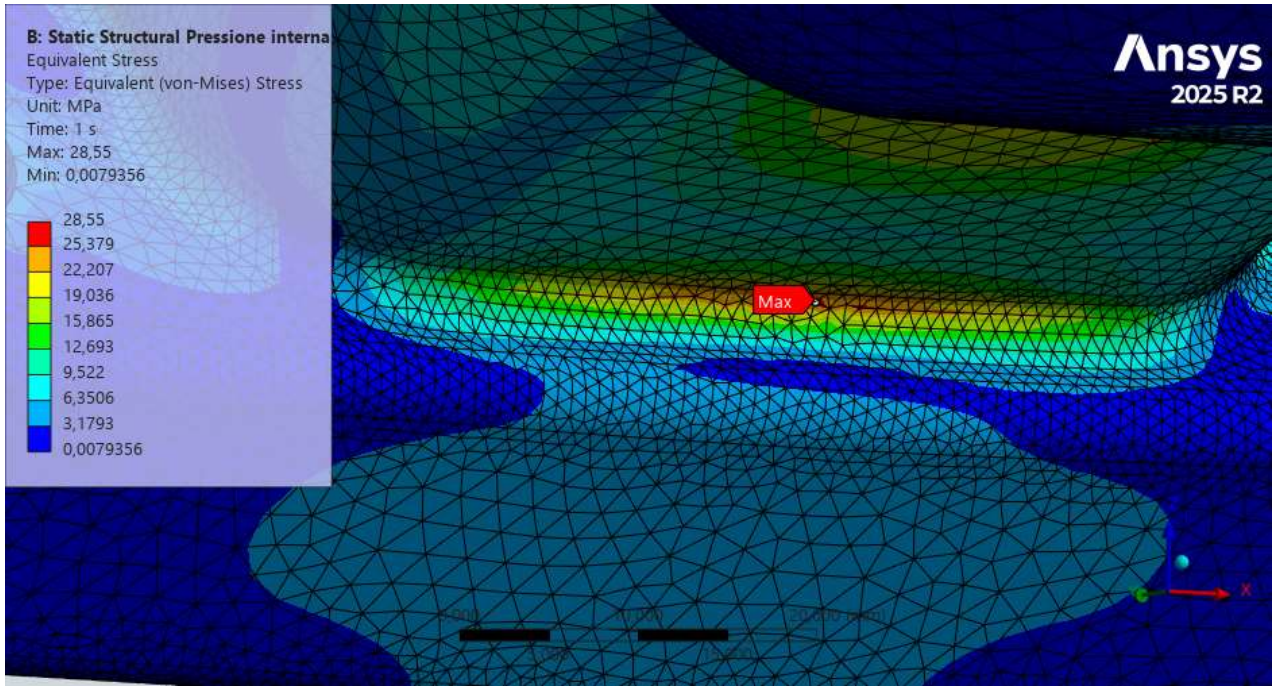

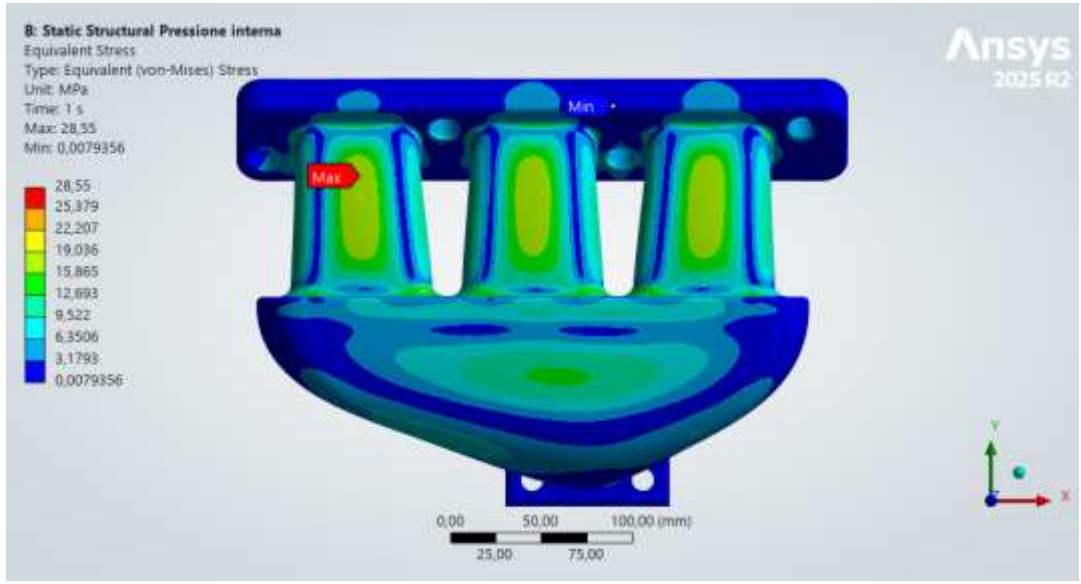

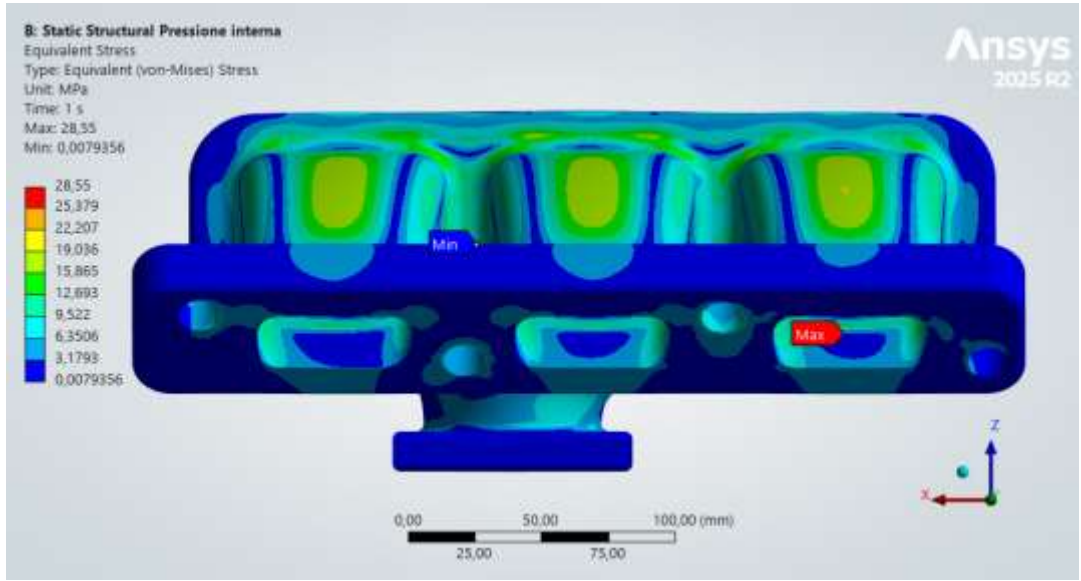

Baseline FEA Results

Stress Analysis: internal pressure of 2.8 Bar

As expected the flange-to-runner region experiences lower stress levels under this loading condition.
Maximum stress of 14.12 MPa

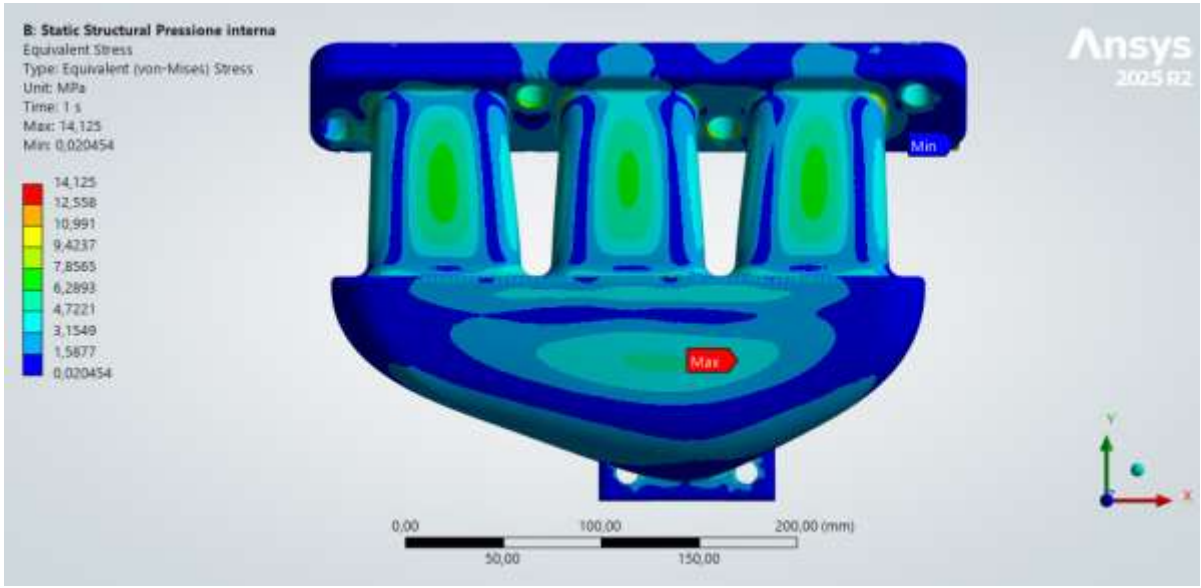

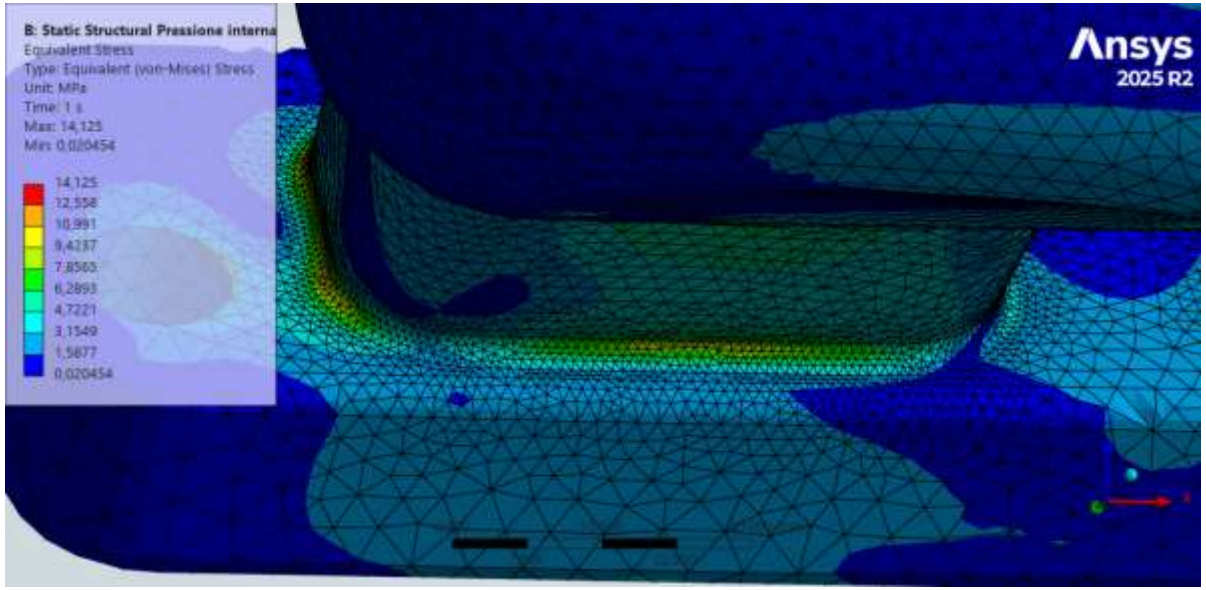

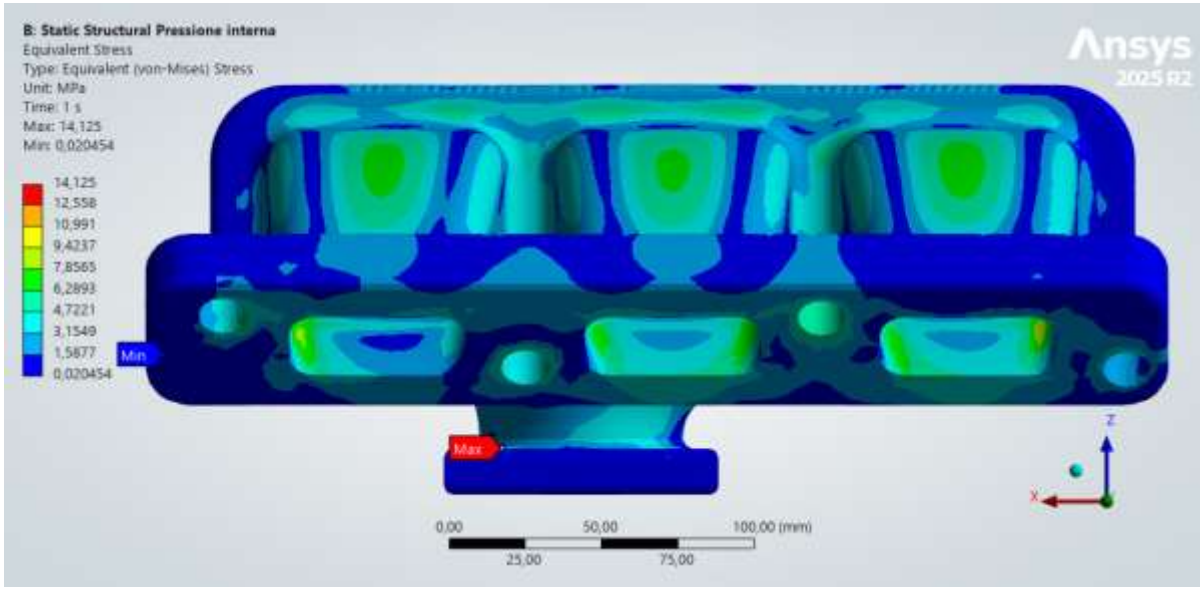

Baseline FEA Results

Linear Buckling Analysis: exteral atmospheric pressure and internal vacuum

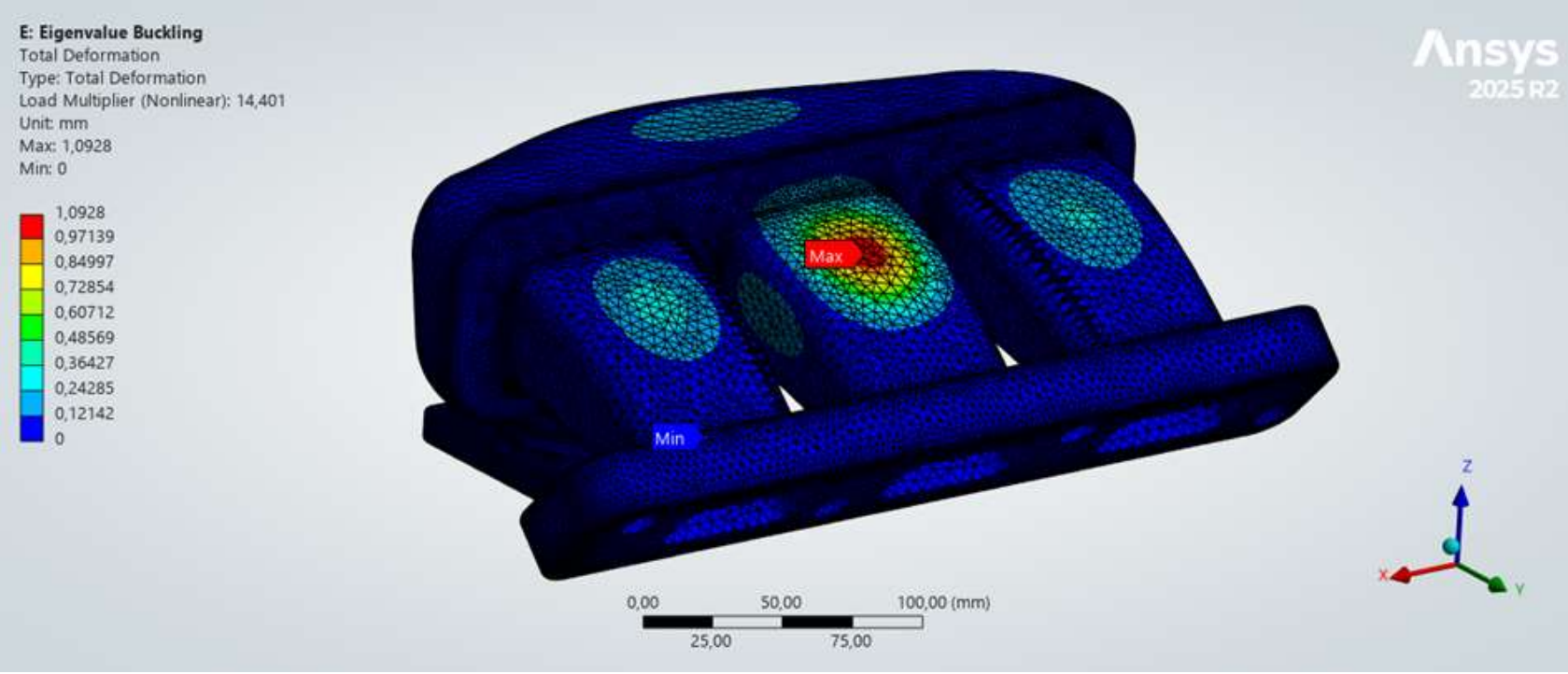

- First buckling mode eigenvalue = 14.40
- An external pressure of approximately 14 Bar is required to trigger buckling instability.

In this loading configuration the component is very far from the buckling condition.

Baseline project objectives

Objective	Value	Limit value	Safety Factor	
Geometric requirements	/	/	/	✓
Pressure proof test	28.55 MPa	32 MPa	1.12 > 1	✓
Buckling resistance	14.40	3	14.40 > 3	✓
Resistance under nominal load	14.12 MPa	32 MPa	2.26 > 2	✓
Total mass	1.23 Kg (-23%)	1.28 Kg	1.23 Kg < 1.28 Kg	✓

Parametric optimization

- **Objective:**

  Reduce component mass while maintaining acceptable stress levels.

- **Parametric optimization:**

  Runner wall thicknesses were modified through surface offsets.

- **RBF Mesh Morphing:**

  RBF Morph integrated within ANSYS Mechanical was used to modify the geometry. Using Radial Basis Function (RBFs), nodal positions were updated without remeshing.

$$\begin{cases} s_x(x) = \sum_{i=0}^{N} {\gamma_i}^x \varphi(\|x - x_i\|) + {\beta_1}^x + {\beta_2}^x x + {\beta_3}^x y + {\beta_4}^x z \\ s_y(x) = \sum_{i=0}^{N} {\gamma_i}^y \varphi(\|x - x_i\|) + {\beta_1}^y + {\beta_2}^y x + {\beta_3}^y y + {\beta_4}^y z \\ s_z(x) = \sum_{i=0}^{N} {\gamma_i}^z \varphi(\|x - x_i\|) + {\beta_1}^z + {\beta_2}^z x + {\beta_3}^z y + {\beta_4}^z z \end{cases}$$

Optimized FEA results

Stress Analysis: internal pressure of 6 Bar

Among all the design points evaluated from the optimizer for the runner surface offsets, two cases were analyzed.

Case 1: offset -0.84mm

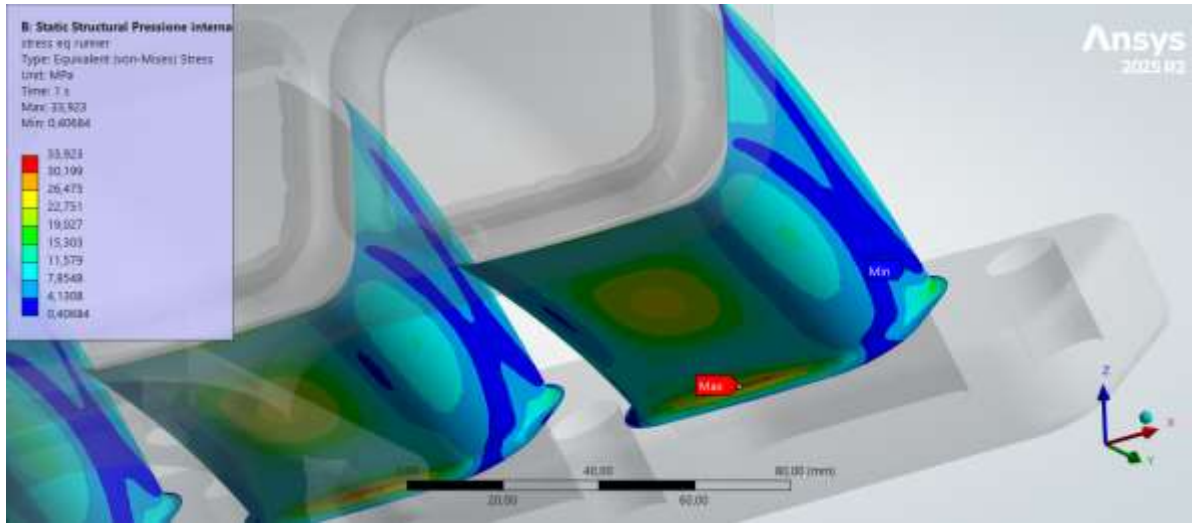

Equivalent maximum stress: 33.92 MPa

Case 2: offset -0.67mm

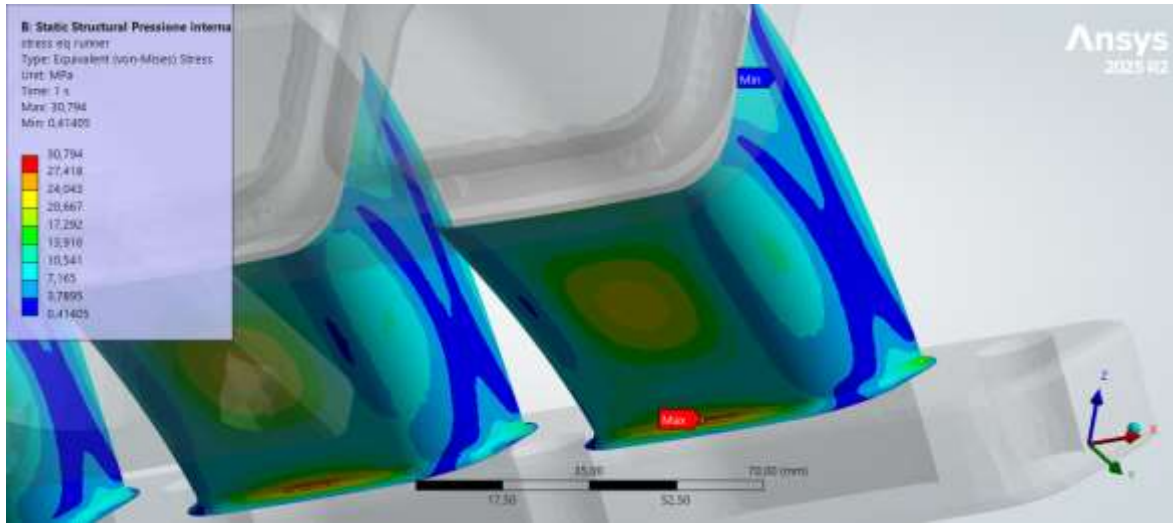

Equivalent maximum stress: 30.79 MPa

Yield Strength at 43°C : 32 MPa

Optimized FEA results

Stress Analysis: internal nominal pressure of 2.8 Bar

Among all the design points evaluated from the optimizer for the runner surface offsets, two cases were analyzed.

Case 1: offset -0.84mm

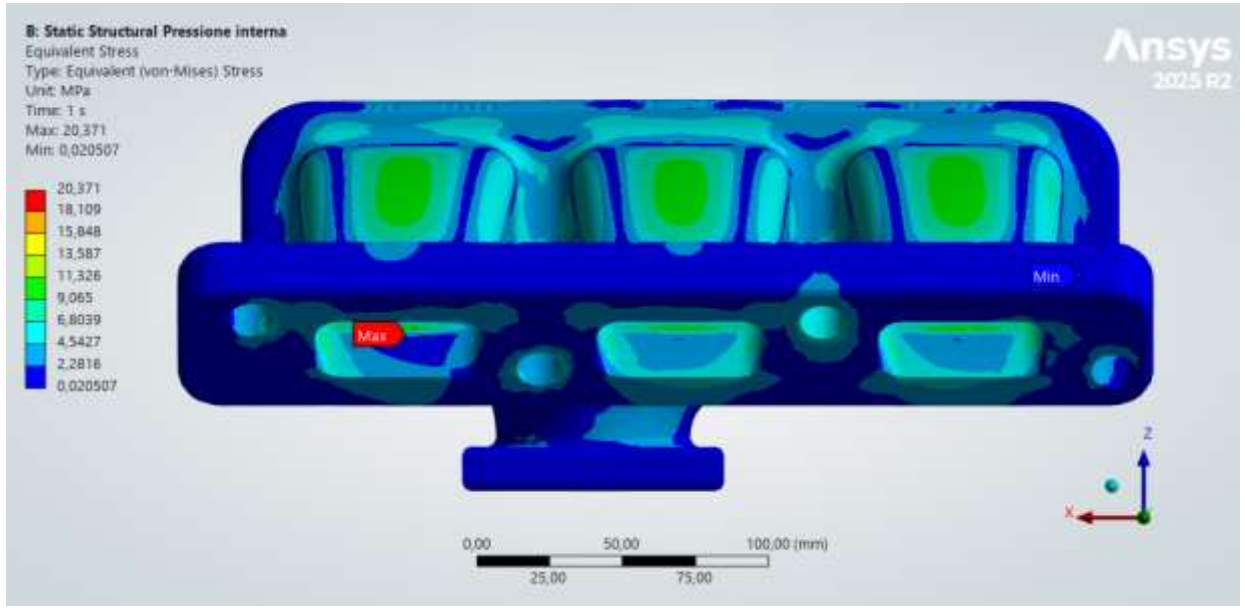

Equivalent maximum stress : 20.37 MPa

Case 2: offset -0.67mm

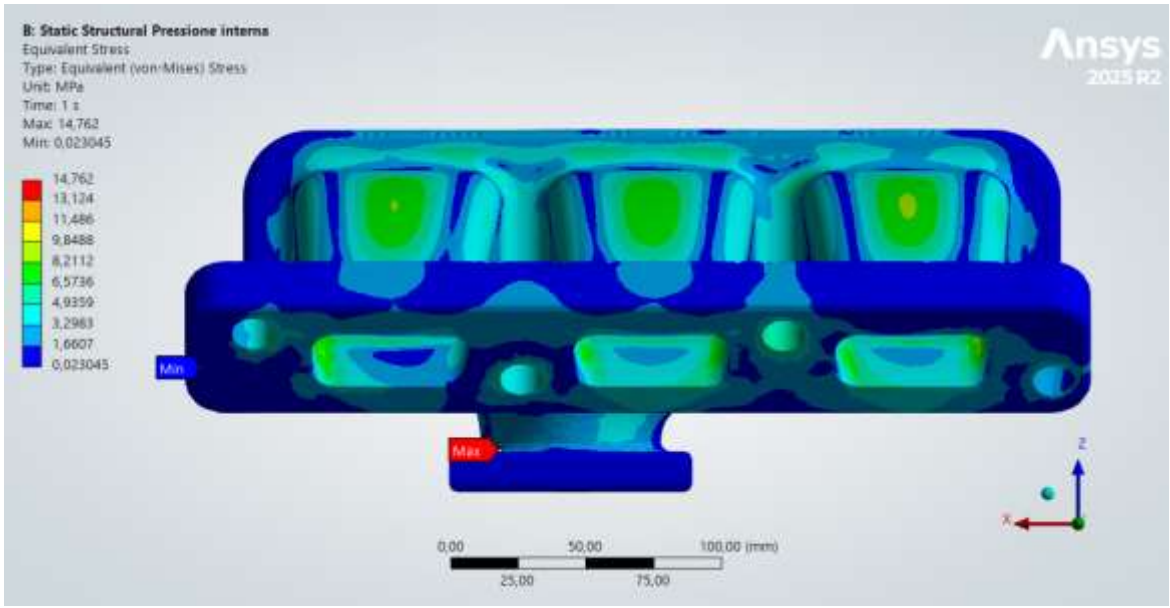

Equivalent maximum stress : 14.76 MPa

Optimized FEA results

Linear Buckling Analysis: atmospheric pressure and internal vacuum

Among all the design points evaluated for the runner surface offsets, two cases were analyzed.

Case 1: offset -0.84mm

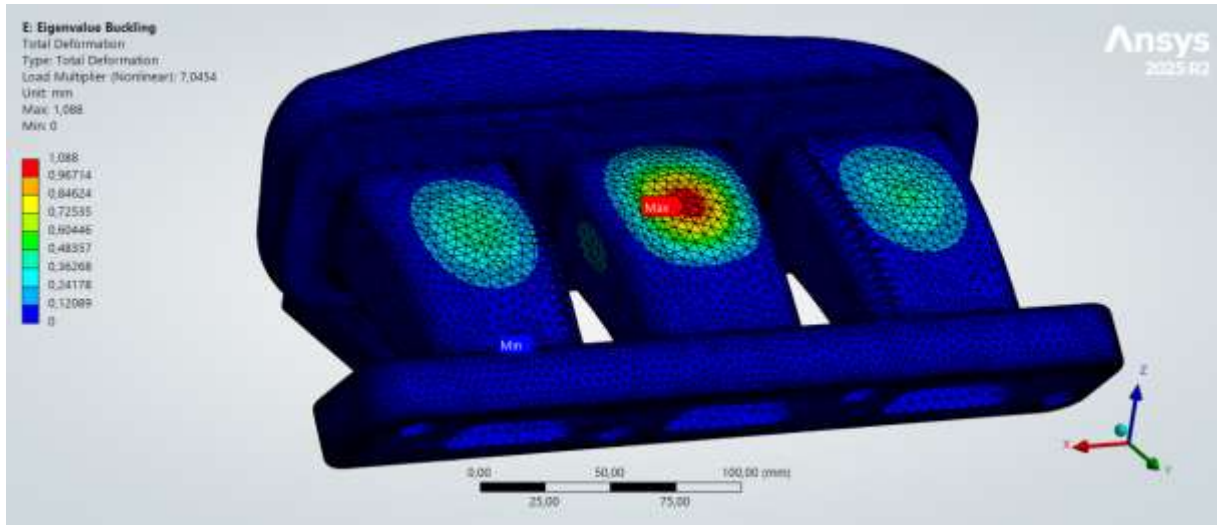

- First buckling mode eigenvalue = 7.04
- Approximately 7 bar of compression are required to initiate buckling

Case 2: offset -0.67mm

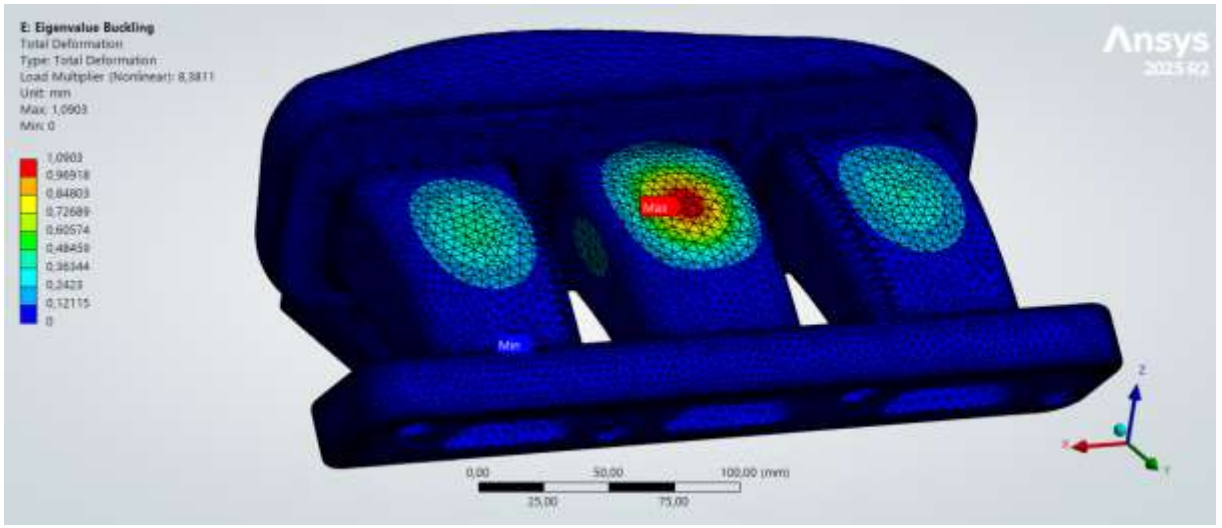

- First buckling mode eigenvalue = 8.38
- Approximately 8 Bar of compression are required to initiate buckling

Optimized design objectives assessment

Objectives 1° (-0,84mm)	Value	Limit value	Safety Factor	
Geometric requirements	/	/	/	✓
Pressure Proof Test	33.92 MPa	32 MPa	0.94 < 1	✗
Buckling resistance	7.04	3	7.04 > 3	✓
Nominal load resistance	20.37 MPa	32 MPa	1.57 < 2	✗
Total mass	1.18 Kg (-26%)	1.28 Kg	1.18 Kg < 1.28 Kg	✓
Objectives 2° (-0,67mm)	**Value**	**Limit value**	**Safety Factor**	
Geometric requirements	/	/	/	✓
Pressure Proof Test	30.79 MPa	32 MPa	1.03 > 1	✓
Buckling resistance	8.38	3	8.38 > 3	✓
Nominal load resistance	14.76 MPa	32 MPa	2.16 > 2	✓
Total mass	1.19 Kg (-25%)	1.28 Kg	1.19 Kg < 1.28 Kg	✓

Conclusions and future developments

This thesis presented the design and optimization process of a high-performance intake manifold.

- A structural verification methodology for an aftermarket automotive intake manifold was developed.
- The partner company's requirements were translated into engineering KPIs and assessed through high-fidelity finite element analyses.
- Mesh morphing techniques enabled weight reduction while maintaining a stress distribution comparable to the baseline design.
- Future developments include the integration of structural and fluid-dynamic optimization to achieve a final design with enhanced functional and structural performance.
- The physical prototype will be manufactured using MJF 3D printing technology.
- Further optimization activities will focus on additional wall-thickness reductions in other manifold regions.

TOR VERGATA

UNIVERSITÀ DEGLI STUDI DI ROMA